

LABORATORY CALIBRATION OF EARTH PRESSURE CELLS

*Chamara Prasad Gunasekara Jayalath¹ and Kasun Dilhara Wimalasena²

^{1,2}School of Civil and Environmental Engineering, Queensland University of Technology, Australia

*Corresponding Author, Received: 27 Nov. 2020, Revised: 13 Jan. 2021, Accepted: 10 Mar. 2021

ABSTRACT: Strain-gauge type soil pressure transducers are widely used in laboratory and field investigation on the performance, and health monitoring of geo-structures to accurately measure the soil pressure. Even though these pressure plates are sold with the factory-measured calibration factors, these sensors should be re-calibrated in the laboratory before using them because the calibration can be affected by the data-logging system and the length of the cable used. Therefore, in this study, a laboratory calibration procedure for strain-gauge type soil pressure plates was proposed. The soil pressure transducer was embedded in a uniform-fine-sand medium in a specially designed pressure cylinder, and the pneumatic pressure was applied into the system as gradual increments. After that, the calibration chart of the pressure gauge was developed based on the sensor outputs for different pressures applied. Then the calibrated soil pressure transducer was used in the laboratory pavement model test to measure soil pressure at the base-subgrade interface under a surface loading area. The measured soil pressure values were compared with the estimated vertical stresses from elastic theories to validate the pressure measurements and the calibration process of the soil pressure transducer. Test results revealed that there is a satisfactory agreement between the pressure measured by the soil pressure transducer and theoretical estimations. Thus, the calibration process of the soil pressure transducer and its outputs are proven to be accurate.

Keywords: Vertical stress in soil, Geotechnical Instrumentation, Pavement subgrade, Soil pressure transducers

1. INTRODUCTION

Well-constructed and maintained geotechnical structures are crucial for the economy of any country. It is mainly because these structures are integral parts of many civil engineering projects related to embankments [1-9], road and railways [10-21], landfills [22,23], coastal protection [24-26] and tunnel construction [30-32]. Therefore, the accurate measurement of soil or earth pressure is essential in laboratory and field investigation on the performance, and health monitoring of these geo-structures [30-38]. Vibrating wire and strain-gauge type pressure plates are widely used to measure soil pressures. Strain-gauge type soil pressure plates are commonly used in laboratory model tests due to its high accuracy, less sensitivity to temperature, and availability in different sizes. Even though these pressure plates are sold with the factory-measured calibration factors, it is important to re-calibrate these transducers in the laboratory prior using them [39] as the calibration can be affected by several factors such as the data-logging system and the length of the cable used. Therefore, as a common practice, several laboratory methods are used to calibrate soil pressure sensors.

The most common calibration methods of soil pressure cells are Dead Weight Calibration (DWC), fluid/pneumatic calibration and soil calibration. In the DWC method, the calibration is performed by placing known dead weights directly on the sensing

area of the pressure cell in increments. Majority of the researchers prefer to calibrate pressure sensors by DWC method as it is less time consuming, economical and easy to perform without much-advanced equipment and technical experience [40]. Generally, fluid/pneumatic calibration is highly recommended compared to the DWC method as the former method provides more accurate results [41]. In this method, the calibration is performed in a calibration chamber by applying hydrostatic or air pressure in increments. However, this method demands advanced laboratory facilities and technical knowledge, which are not available in most laboratories. As an alternative, the soil-calibration method can be used in the laboratory to calibrate soil pressure cells. Therefore, in this study, a laboratory calibration procedure for strain-gauge type soil pressure plates using sand is proposed. Then the calibrated soil pressure transducer was used in a laboratory pavement model test to measure soil pressure at subgrade-base interface under a circular-area loading applied on the top surface. The measured soil pressures were compared with the estimated vertical stresses from elastic theories to validate the pressure measurements and the calibration process of the soil pressure transducer.

2. SOIL PRESSURE TRANSDUCER

A soil pressure transducer (See Fig.1) with 1MPa capacity was used in this experimental study.

The outside diameter and the thickness of the pressure plate are 200mm and 25.5mm, respectively. The percentage of rated output (%RO) of the pressure gauge has been specified as 1%, and the diameter of the sensing area is 166mm. It is designed with a dual-diaphragm structure that can minimise the displacement of a sensing area, and thereby can keep the stress distribution undisturbed under pressure. This type of soil pressure gauges is widely used to measure the pressure in soil and to monitor the behaviour of embankments.



Fig.1 Soil pressure transducer

3. METHODOLOGY

A specially designed pressure cylinder [42, 43] (See Fig.2 (a)) made of acrylic was used to calibrate the soil pressure transducers. The internal diameter and the height of the cylinder are 360mm and 400mm respectively. A uniform-fine sand was used in this calibration. The particle size distribution and properties of the sand are given in Fig.3 and Table 1, respectively. The sand was filled up to 250mm, and the sand surface was properly levelled. Thereafter, the soil pressure transducer was placed on top of the sand layer. The level of the top surface of the sensor was checked with a spirit level (bubble level), as shown in Fig.2 (b). Then the sand was filled to have a 50mm thick sand layer above the top of the sensor. The sand surface was levelled, and the inner wall of the cylinder was cleaned to remove all the attached sand and dust. Lubricating oil was applied on the inner wall of the cylinder to minimise the friction between the wall and the piston. After that, the piston was placed inside the cylinder and valves were connected to supply the pneumatic pressure into the setup.

A pressure above 750kPa (i.e. 785kPa) was applied into the setup for 24 hours to allow the particle rearrangement of the sand under high pressures. From the initial trials conducted prior to this experiment, it was found that the required pressure to overcome the friction between the piston and the wall of the cylinder is negligible. Since the sand thickness above the top surface of the sensor is thin (i.e. 50mm), and the friction is negligible, it is

reasonable to assume that the pressure applied on the sensor is equal to the applied pressure into the setup. The pressure into the system was increased approximately up to 750kPa in 50kPa increments. The pressure gauge was connected to a data logger, and the sensor readings were recorded in parts per million (ppm) for each pressure increment. Based on the sensor outputs for different applied pressures, the calibration chart of the pressure gauge was developed.

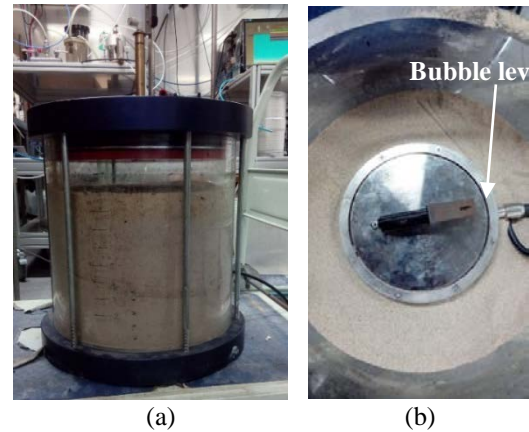


Fig.2 calibration of soil pressure transducers; (a) The pressure cylinder; (b) Embedding the soil pressure transducer in the cylinder

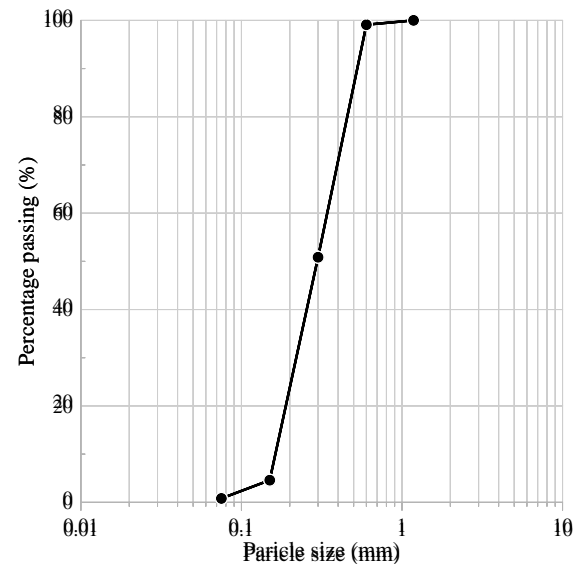


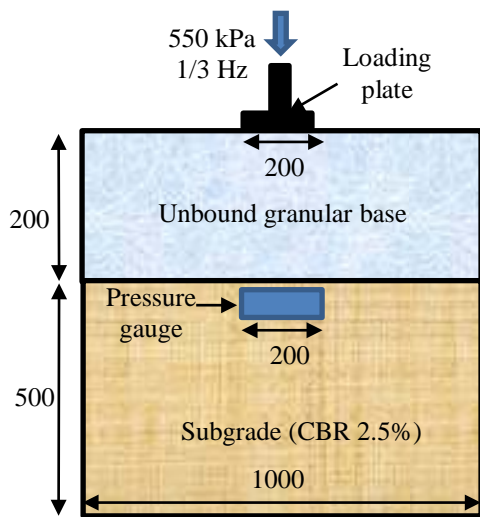
Fig.3 Particle size distribution of sand used in the calibration of soil pressure transducers

This soil pressure transducer was used to measure the pressure applied at the base-subgrade interface of unbound-granular pavement-models during a cyclic loading test series. The schematic diagram of the experimental setup of the cyclic-loading pavement test is shown in Fig.4. A granular

pavement with 200mm unbound-granular base and 500mm thick subgrade with 2.5% unsoaked-CBR was selected in the present study to verify the pressure measurements given by the pressure gauge. The pressure gauge was embedded in the subgrade close to the base-subgrade interface and below the centre of the loading area as shown in Fig.5. In this experiment, the maximum load of 17.31kN was applied through a 25mm thick and 200mm diameter steel plate to create a tyre-contact pressure of 550kPa with a frequency of 0.33Hz. More details of the conducted test can be found in [44] and [45]. The pressure sensor was connected to the data logger, and the readings were recorder for every five seconds. After that, the captured sensor outputs were converted to pressure readings using the developed calibration equation.

Table 1 Properties of sand used in the calibration of soil pressure transducers

Property	Value
D ₁₀ (mm)	0.165
D ₃₀ (mm)	0.220
D ₆₀ (mm)	0.340
Coefficient of curvature (Cc)	2.06
Coefficient of uniformity (Cu)	0.86



Note: Not to scale
All dimensions are in millimetres

Fig.4 The schematic diagram of the experimental setup of the cyclic-loading pavement test

The measured soil pressure values were compared with the calculated values from two elastic-theories methods, namely Boussinesq

method [46] and Fox L. method [47], to validate the measured values and the calibration process of the soil pressure gauge. Even though Boussinesq equation for vertical stresses under uniformly loaded circular area has been derived for homogeneous, elastic, and isotropic mediums, it was used for this two-layer system for a rough estimation of vertical stresses at the base-subgrade interface. In addition, the pressure applied at the base-subgrade interface was also computed based on the chart for the vertical stresses on the interface stresses developed by Fox L. method.



Fig.5 Installation of the soil pressure transducer

4. RESULTS AND DISCUSSION

The applied vertical pressure values were plotted against the corresponding sensor readings to develop the calibration chart of the soil pressure transducer, as shown in Fig.6. The equation for the regression line of the plotted points was adopted as the calibration equation of the sensor. The obtained calibration equation perfectly fits the data as the coefficient of determination is equal to one ($R^2=1$). Later, this calibration equation was utilised to determine the vertical stresses applied at the base-subgrade interface of the laboratory-scale unbound-granular-pavement model.

In a previous experimental study, two tactile pressure sensors of dimensions of 25 mm × 25 mm × 2 mm with 345 kPa capacity were calibrated using the DWC and fluid calibration methods. The R^2 values of the non-linear calibration curves obtained from the DWC method have been reported as 0.992 and 0.998 [40]. During the fluid calibration, the observed output voltage from a tactile pressure sensor for applied pressure was much lesser compared to that of DWC results. An R^2 value has not been calculated/mentioned for the calibration equation obtained from the fluid calibration method.

Fig.7 illustrates the variation of the vertical stress

at the base-subgrade interface of the laboratory-scale unbound-granular-pavement model. Three curves were produced depending on the technique (e.g. pressure gauge, Boussinesq method and Fox L. method) used to measure/estimate vertical stresses during the test. All three curves were plotted approximately up to 120,000 cycles where the cycling loading test was stopped. Results show that estimated vertical stresses from the Boussinesq method are always higher than Fox L. method. Soon after the commencement of the loading, the vertical stress applied at the base-subgrade interface was measured as 170kPa whereas estimated stresses were 169kPa and 144kPa respectively from the Boussinesq equation and Fox L. method. The measured vertical stresses follow the similar shape and magnitudes of the vertical stress development computed by Boussinesq method in the initial stage of the test, approximately up to 27,000 cycles where the measured vertical stress lies at 260kPa. Then, measured vertical stresses by the soil pressure transducer fluctuate in between the vertical stress values estimated by the two elastic-theory methods up to 100,000 cycles, afterwards, follow the similar shape and magnitudes of the vertical stress variation estimated by Fox L. method until the end of the test where the measured vertical stress was 313kPa.

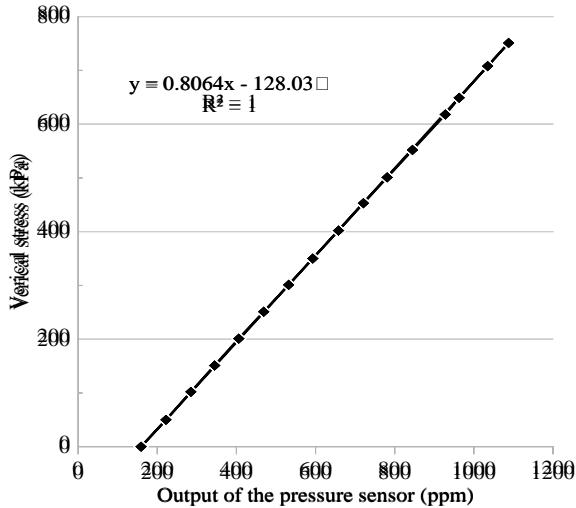


Fig.6 Calibration chart of the soil pressure transducer

As mentioned in the methodology section, Boussinesq equation has been developed to estimate vertical stresses of homogeneous, elastic and isotropic mediums but the tested pavement section has two layers (i.e. subgrade layer and granular base layer) which have completely different material properties. Each layer alone can be considered as homogeneous and elastic; however, both subgrade and granular materials are cross-

anisotropic. The referred chart from Fox L. method for the vertical stresses on the interface has been developed for two-layer pavement systems considering the influence of the ratio of the elastic modulus of the top and the bottom layers (E_1/E_2). As the subgrade CBR value is 2.5%, the elastic modulus of the subgrade was estimated to be 25MPa based on the approximation that elastic modulus of pavement material is ten times its CBR value as specified in Austroads Guide to Pavement Technology Part 2: Pavement Structural Design [48]. Based on the mechanistic-pavement design principals, the average elastic modulus of the granular base, which was limited by the weak subgrade was estimated as 51MPa. Therefore, the E_1/E_2 of the tested pavement section is approximately two (i.e. $E_1/E_2 = 2$). However, in the Boussinesq case, E_1/E_2 ratio must be assumed as one (i.e. $E_1/E_2 = 1$) even when it is used for a two-layer system. These assumptions may result in slight differences between the actual pressure measurements and estimated vertical stresses from methods based on the elastic theory. Overall, it is evident that a reasonable agreement between the pressures measured by the sensor and the theoretical estimations is apparent. Thus, the calibration process of the soil pressure transducer and its outputs are proven to be accurate. Therefore, the proposed calibration method can be used to calibrate soil pressure cells in the laboratory accurately.

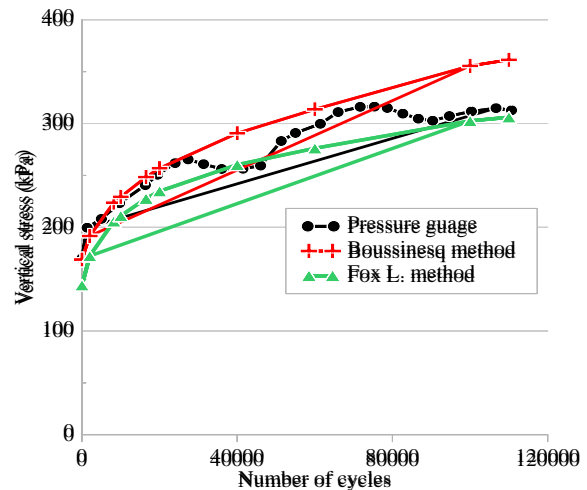


Fig.7 Development of the vertical stress at the base-subgrade interface

5. CONCLUSION

Based on the test results of the calibration of the pressure transducer and the comparison of measured pressures with theoretical estimations, the following conclusions can be drawn:

•The developed calibration equation perfectly fits the data as the coefficient of determination is equal to one ($R^2=1$); therefore, it can be assumed as accurate.

•A satisfactory agreement between the sensor measurements and theoretical estimations is evident. Thus, the calibration process of the soil pressure transducer and its outputs are proven to be accurate.

•The presented calibration method can be effectively used as a laboratory calibration methodology to calibrate soil pressure cells accurately.

6. ACKNOWLEDGMENTS

The authors acknowledge the continued support of the Department of Transport and Main Roads (TMR) and Australian Road Research Board (ARRB) by providing the required funding for the instruments including data logger and pressure sensors for this research study and supplying the required testing materials. Thanks are also extended to the technical staff of Banyo Pilot Plant Precinct of Queensland University of Technology (QUT) for their great support and assistance during the pavement model test. Further, the first author would like to thank his colleagues and friends who helped in preparing the pavement model, and for QUT for providing him with a scholarship to pursue his postgraduate studies.

7. REFERENCES

- [1] Suryo E., Zaika Y., Gallage C. and Trigunaryyah, B., A non-destructive method for investigating soil layers of an individual vulnerable slope, *International journal of GEOMATE*, 18(69), 2020, pp. 1-8.
- [2] Abeykoon A., Gallage C. P., Dareeju B. S. and Trofimovs J., Real-time monitoring and wireless data transmission to predict rain-induced landslides in critical slopes, *Australian Geomechanics Journal*, 53 (3), 2018, pp. 61-76.
- [3] Garcia E. F., Gallage C. and Uchimura T., Function of permeable geosynthetics in unsaturated embankments subjected to rainfall infiltration, *Geosynthetics International*, 14 (2), 2018, pp. 89-99.
- [4] Gallage C. P., Dareeju B. S., Trofimovs J., Wang L. and Uchimura T., Real-time monitoring and failure prediction of a slope due to rainfall-case study, *Proceedings of the 9th International Conference on Sustainable Built Environment 2018 (ICSBE)*, 2018, pp. 12-18.
- [5] Suryo E., Gallage C. P. and Trigunaryyah B., A method for predicting rain-induced instability of an individual slope, *Proceedings of the 9th Annual International Conference of the International Institute for Infrastructure Renewal and Reconstruction*, 2015, pp. 118-127.
- [6] Gallage C. P. and Uchimura T., Investigation on parameters used in warning systems for rain-induced embankment instability, *Proceedings from the 63rd Canadian Geotechnical Conference (GEO2010)*, 2010, pp. 1025-1031.
- [7] Gallage C. P. K., Garcia, E. and Uchimura T. Stability a model embankment subjected to an artificial rainfall, *Proceedings of The Second Japan -Taiwan Joint Workshop on Geotechnical Hazards from Large Earthquakes and Heavy Rainfall*, Nagaoka, Niigata, Japan, 2006.
- [8] Garcia E. F., Gallage C. P. K. and Uchimura T., Unsaturated infiltration on artificial embankments reinforced with geosynthetics. *Proceedings of the 8th International Conference on Geosynthetics*, Yokohama, Japan, 2006.
- [9] Gallage C., Garcia E., Peiris A., Uchimura T. and Ochiai H., Use of soil-water characteristics curve in determination of stability of embankments during drying and wetting processes, in *Advanced experimental unsaturated soil mechanics: Proceedings of the International Symposium on Advanced Experimental Unsaturated Soil Mechanics 2005*, Italy, Trento, 2005, pp. 351-358.
- [10] Clark B. R. and Gallage C., Superior performance benefits of multigrade bitumen asphalt with recycled asphalt pavement additive. *Construction and Building Materials*, 230, Article number-116963, 2020, 10.1016/j.conbuildmat.2019.116963.
- [11] Clark B. R., Gallage C. and Yeaman J., Temperature variation through Deep Multigrade Asphalt Pavements and Proposed Method for Accounting for Fluctuations. *Journal of Materials in Civil Engineering*, 32(3), 2020, [https://doi.org/10.1061/\(ASCE\)MT.1943-5533.0003059](https://doi.org/10.1061/(ASCE)MT.1943-5533.0003059)
- [12] Jayakody S., Gallage, C and Ramanujam J., Effects of reclaimed asphalt materials on geotechnical characteristics of recycled concrete aggregates as a pavement material. *Road Materials and Pavement Design*, 20(4), 2019, pp. 754-772.
- [13] Jayakody S., Gallage C. and Ramanujam J. [2019] Performance characteristics of recycled concrete aggregates as an unbound pavement material, *Heliyon*, 9 (5), 2019, <https://doi.org/10.1016/j.heliyon.2019.e02494>
- [14] Jayakody A. S., Gallage C. P. and Ramanujam J. M., Effects of reclaimed asphalt materials on geotechnical characteristics of recycled concrete aggregates as a pavement material, *Road Materials and Pavement Design*, 20 (4),

- 2019, pp. 754-772.
- [15] Askarinejad H., Barati P., Dhanasekar M. and Gallage C. P., Field studies on sleeper deflection and ballast pressure in heavy haul track, *Australian Journal of Structural Engineering*, 19 (2), 2018, pp. 96-104.
- [16] Dareeju B. S., Gallage C. P., Ishikawa T., Dhanasekar M. and Dawes L. A., Effects of particle size distributions and principal stress axis rotation on cyclic plastic deformation characteristics of coarse materials, *Journal of GeoEngineering*, 13 (4), 2018, pp. 161-170.
- [17] Clark B. R., Gallage C. P. and Yeahman J., Temperature susceptibility of multigrade bitumen asphalt and an approach to account for temperature variation through deep pavements, *International Journal of Urban and Civil Engineering (World Academy of Science, Engineering and Technology)*, 12 (6), 2018, pp. 712-717.
- [18] Clark B. R., Piacere L. and Gallage C. P., Effects of recycled asphalt pavement on the stiffness and fatigue performance of multigrade bitumen asphalt, *Journal of Materials in Civil Engineering*, 30 (2), 2018, pp. 1-8.
- [19] Dareeju B., Gallage C. P., Ishikawa T. and Dhanasekar M., Effects of principal stress axis rotation on cyclic deformation characteristics of rail track subgrade materials, *Soils and Foundations*, 57 (3), 2017, pp. 423-438.
- [20] Gallage C. P., Dareeju B., Dhanasekar M. and Ishikawa T., Effects of principal stress axis rotation on unsaturated rail track foundation deterioration, *Procedia Engineering*, 143, 2016, pp. 252-259.
- [21] Gallage C. P., Eom T., Barker D. and Ramanujam J., Falling Weight Deflectometer (FWD) tests on granular pavement reinforced with geogrids - Case study, *Geotechnics for Sustainable Development: Proceedings of the 2015 International Conference on Geotechnical Engineering (ICGE)*, 2015, pp. 597-600.
- [22] Weerasinghe, I., Gallage, C., Dawes, L. and Kendall, P., Factors affecting the hydraulic performance of a Geosynthetic clay liner overlap. *Journal of Environmental Management*, 2020, <https://doi.org/10.1016/j.jenvman.2020.110978>
- [23] Weerasinghe I. A., Gallage C. P. and Dawes L. A., Optimising geosynthetic clay liner overlaps: Implications on hydraulic performance, *Environmental Geotechnics*, Online (Online), 2019, pp. 1-43.
- [24] Cheah C., Gallage C. P., Dawes L. A. and Kendall P., Measuring hydraulic properties of geotextiles after installation damage, *Geotextiles and Geomembranes*, 45 (5), 2017, pp. 462-470.
- [25] Cheah C., Gallage C. P., Dawes L. A. and Kendall P., Impact resistance and evaluation of retained strength on geotextiles, *Geotextiles and Geomembranes*, 44 (4), 2016, pp. 549-556.
- [26] Cheah C., Gallage C., Dawes L. A. and Kendall, P. Effect of simulated rock dumping on geotextile. In Ramsay, Graham (Ed.) 12th Australian New Zealand Conference on Geomechanics (ANZ 2015), 22-25 February 2015, Wellington, New Zealand, 2015.
- [27] Koneshwaran S., Thambiratnam D. P. and Gallage C. P., Performance of buried tunnels subjected to surface blast incorporating fluid structure interaction, *Journal of Performance of Constructed Facilities*, 29 (3), 2015, pp. 1-70.
- [28] Koneshwaran S., Thambiratnam D. P. and Gallage C. P., Blast response and failure analysis of a segmented buried tunnel, *Structural Engineering International*, 25 (4), 2015 pp. 419-431.
- [29] Koneshwaran S., Thambiratnam D. P. and Gallage C. P., Response of segmented bored transit tunnels to surface blast, *Advances in Engineering Software: including computing systems in engineering*, 89, 2015, pp. 77-89.
- [30] Gallage C., Kodikara J. K. and Chan D., Response of a plastic pipe buried in expansive clay, *Proceedings of the Institution of Civil Engineers: Geotechnical Engineering*, 165 (1), 2012, pp. 45-57.
- [31] Chan D., Gallage C. P., Rajeev P. and Kodikara J.K., Field performance of in-service cast iron water reticulation pipe buried in reactive clay, *Canadian Geotechnical Journal*, 52 (11), 2015, pp. 1861-1873.
- [32] Chan D., Rajeev P., Kodikara J.K. and Gallage C. P., Field performance of in-service cast iron gas reticulation pipe buried in reactive clay, *Journal of Pipeline Systems Engineering and Practice*, 7 (2), 2016, pp.1-15
- [33] Chan D., Gallage C., Gould S., Kodikara J.K., Bouazza A. and Cull J., Field instrumentation of water reticulation pipe buried in reactive soil, In *Ozwater'09 : Australia's National Water Conference and Exhibition*, Melbourne, Victoria, Australia, 2009, pp. 9-16.
- [34] Gallage C. P., Kodikara J. K., Chan D. and Davis P., A comparison of the results of the numerical analysis and the physical behaviour of a pipe buried in reactive clay, in *Proceedings of the 12th International Conference of the Association for Computer Methods and Advances in Geomechanics (IACMAG)*, 2008, pp. 1-9.
- [35] Kodikara J., Davis P., Gallage C., Chan D., Gould S. and Zaho X.L., Behaviour of a polyethylene pipe buried in reactive soil. *Proceedings of the 7th National ASTT Conference*, Sydney, Australia, 2008 (CD Rom publication).

- [36] Gallage C., Chan D., Gould S. and Kodikara J. K., Behaviour of an in-service cast iron water reticulation pipe buried in expansive soil, In Ozwater'09: Australia's National Water Conference and Exhibition, 16-18 March, 2009, Melbourne, Victoria, Australia, 2009, pp. 1-8.
- [37] Gallage C. P., Chan D., Kodikara, J. K. and Ng P. C., Discussion: Response of a plastic pipe buried in expansive clay, Proceedings of the Institution of Civil Engineers: Geotechnical Engineering, 166 (3), 2013, pp. 328- 330.
- [38] Gallage C., Gould S., Chan D., Kodikara J., Field measurement of the behaviour of an in-service water reticulation pipe buried in reactive soil (Altona North, Victoria), Monash University, Australia, Research report RR10. 2008.
- [39] Chen Q., Abu-Farsakh M., and Tao M., Laboratory evaluation of geogrid base reinforcement and corresponding instrumentation program. Geotechnical testing journal, 32(6), 2009, pp. 516-525.
- [40] Gade V. K., and Dasaka S., Calibration of Earth Pressure Sensors. Indian Geotechnical Journal, 2017, pp. 1-11.
- [41] Ramírez A., Nielsen J. and Ayuga, F., On the use of plate-type normal pressure cells in silos: Part 2: Validation for pressure measurements. Computers and electronics in agriculture, 71(1), 2010, pp. 64-70.
- [42] Gallage C. P., Mostofa M., Vosolo D. A. and Rajapakse J. P., A new laboratory model of a slaking chamber to predict the stability of on-site coal mine spoils, International Journal of GEOMATE, 10 (22), 2016, pp. 2065-2070.
- [43] Gallage C. P., Mostofa M., Vosolo D.A. and Rajapakse J.P., Laboratory investigation on the effects of overburden pressure, water, and time on slaking induced material property degradation of coal mine spoil, Geotechnique, Construction Materials and Environment, 2015, pp. 395-400.
- [44] Jayalath. C. P. G, Gallage C., Dhanasekar M., Dareeju B., Ramanujam J., and Lee J. Pavement model tests to investigate the effects of geogrid as subgrade reinforcement. In Liu, H, Mills, P, Ruxton, N, & Mazengarb, C (Eds.) Proceedings of the 12th Australian and New Zealand Young Geotechnical Professionals Conference. Australian Geomechanics Society, Australia, 2018, pp. 1-8.
- [45] Wimalasena K. and Jayalath C. P. G., Effect of geogrid reinforcement in weak subgrades. International Journal of GEOMATE, 18(65), 2020, pp. 140-146.
- [46] Boussinesq J., Application des Potentials à L'Etude de L'Equilibre et du Mouvement des Solides Elastiques, Gauthier-Villars, Paris, 1883.
- [47] Fox L., Computation of traffic stresses in a simple road structure, Proc. 2nd ICSMFE, 1948, 1, 1948, pp. 236-246
- [48] Austroads Guide to Pavement Technology Part 2: Pavement Structural Design. Austroads Inc.: Sydney, Australia, 2012.

Copyright © Int. J. of GEOMATE. All rights reserved, including the making of copies unless permission is obtained from the copyright proprietors.
